

Fatigue Crack Nuclei in Austempered Ductile Cast Iron

T.J. Marrow¹, H. Çetinel², M. Al-Zalmah³

¹ Manchester Materials Science Centre, UMIST, P.O. Box 88, Manchester, M60 1QD, UK.

² Dokuz Eylül University, Faculty of Engineering, Department of Metallurgical and Materials Engineering, Bornova, 35100, İzmir, Turkey.

³ University of Aleppo, Faculty of Engineering, Department of Applied Mechanics, Aleppo, Syria.

ABSTRACT: *Short fatigue crack nuclei in austempered ductile cast iron have been studied using optical microscopy, scanning electron microscopy, electron backscatter diffraction analysis and X-ray microtomography. The aim of the investigation was to determine the mechanisms of crack initiation, propagation and arrest, with the objective of developing a microstructure fracture mechanics model for the statistical distribution of the fatigue endurance limit.*

Short fatigue cracks nucleate at graphite nodules in rising load fatigue tests. The crack nuclei are arrested and retarded by barriers in the microstructure, by either blocking of slip at phase boundaries or the requirement for tilt and twist of the {111} crystallographic crack at the prior austenite grain boundaries. The most significant barriers are the prior austenite grain boundaries. The size of the defects such as graphite nodules and porosity and the size of the prior austenite grains control the largest crack nucleus that can develop, and hence determine the fatigue limit.

INTRODUCTION

The fatigue behaviour of austempered ductile cast iron has been examined in terms of the microstructure short crack mechanisms. Previous observations in an austempered ductile cast iron [1-3] showed a strong correlation between the length of stable crack nuclei from defects and the length of the ferrite laths in the ausferrite microstructure, which were equivalent to the prior austenite grain size (Figure 1) of approximately 25 μm . Fractography and X-ray microtomography [3] showed an inclined and faceted region adjacent to nucleating defects (Figure 2), which was of the order of the austenite grain size and the maximum ausferrite packet size. These crack nuclei were shown to be stable below the fatigue limit.

Electron backscatter diffraction (EBSD) measurements of grain crystallographic orientation (Figure 3) at stable crack nuclei confirmed that the cracks were parallel to the austenite $\{111\}$ plane, which implies that the facets were due to stage I crack nuclei [3]. EBSD was also used to demonstrate that cracks were retarded and arrested at ausferrite packet boundaries and austenite grain boundaries. This may be due to blockage of slip and the requirement for tilt/twist of the crack plane to maintain stage I crack propagation. Atomic force microscopy of the surface deformation associated with arrested cracks found no evidence for martensite transformation as an arrest mechanism for short cracks [3].

These observations indicate that for cracks nucleated at graphite nodules, the maximum crack nucleus size depends on the nodule diameter and the ausferrite matrix microstructure. This observation may be used to model the fatigue limit.

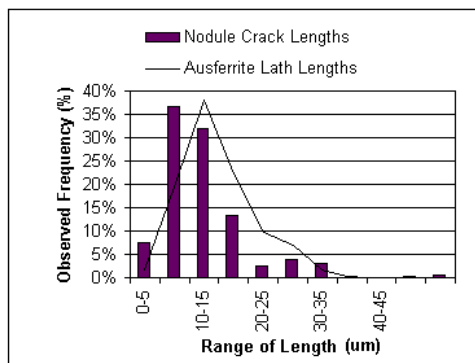


Figure 1: Distribution of stable crack nucleus length below the fatigue limit and the distribution of ausferrite lath lengths [1]. The maximum crack length observed was $55\mu\text{m}$. All cracks were nucleated at graphite nodules.

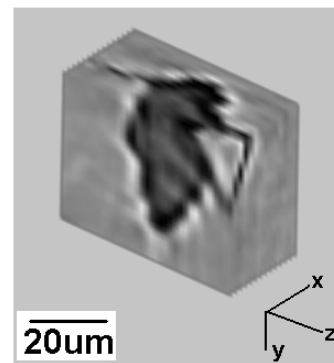


Figure 2: High resolution X-ray tomographic image of an arrested crack nucleus [3]. The inclined plane of the crack nucleus is observed. The stress amplitude was parallel to the X direction.

A MODEL FOR THE FATIGUE LIMIT

A simple linear elastic fracture mechanics model for the relationship between microstructure and the fatigue limit in austempered ductile cast iron is proposed. A critical stress intensity factor range, ΔK_{th} , which must be exceeded for the crack nucleus to propagate, describes the strength of the prior austenite grain boundary barriers. The stress intensity factor for a

crack adjacent to a spherical stress concentration [4] was calculated for a crack of length a , extending from a nodule of radius r using equations (1) and (2), subjected to tension-tension cyclic stress amplitude $\Delta\sigma$.

$$\Delta K = k_i \frac{\pi}{2} (2\Delta\sigma) \sqrt{\pi(a + 2r)} \quad (1)$$

$$k_i = 1 + 1.11 \exp\left(-3.3 \frac{a}{r}\right) \quad (2)$$

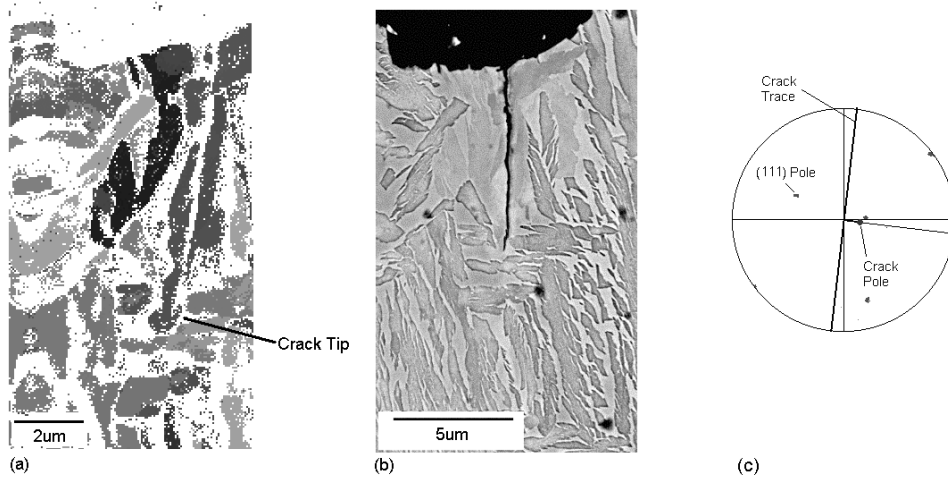


Figure 3: Determination of the retained austenite crystallographic orientation for an arrested crack nucleus using electron backscatter diffraction (EBSD) [3]. The angle of the crack plane was measured by serial sectioning. The crack was nucleated at a graphite nodule. (a) EBSD map, (b) SEM image, (c) Stereographic projection of {111} austenite poles and crack plane.

Figure 4 shows the critical stress amplitude to exceed ΔK_{th} for a crack that propagates from a 45 µm radius nodule. The interaction between increasing stress intensity factor and decreasing stress concentration gives a maximum critical stress amplitude of 160 MPa approximately 40 µm from the nodule. The position of this critical stress amplitude maximum increases proportionally with the nodule radius, and the distance to the maximum is approximately equivalent to the nodule radius. In a material that behaves as a homogeneous continuum, this critical stress amplitude maximum would be the fatigue limit. However, the crack size is

comparable to the microstructure scale, and the discrete nature of the barriers in this heterogeneous material must be considered.

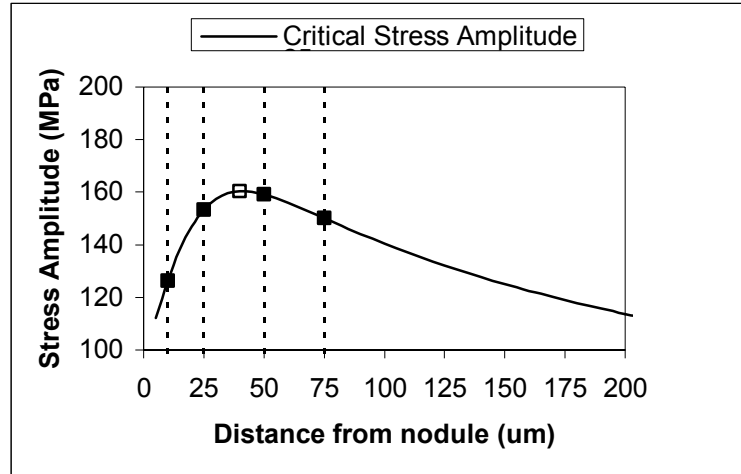


Figure 4: The stress required to exceed the threshold value of ΔK_{th} , as a function of the distance of the crack tip from the nodule. The data is for a 45 μm radius nodule, with a threshold ΔK_{th} of 4.2 $\text{MPa}\sqrt{\text{m}}$.

In a material that contains many crack nuclei, failure will result from the weakest link, i.e. the combination of a graphite nodule and crack length at the grain boundary that becomes unstable at the lowest stress amplitude. For example, in a material with a maximum grain size of 50 μm , the lowest stress amplitude necessary to cross the first microstructure barrier occurs when the grain boundary is at the maximum possible distance of 50 μm (Figure 4). This is beyond the stress amplitude maximum and results in a fatigue limit that is lower than 160 MPa. Grain boundaries that lie closer to nodules of the same radius can arrest crack propagation, producing stable crack nuclei. Increasing the grain size, e.g. to 75 μm , will further decrease the fatigue limit.

With decreasing grain size, the relative size of the grains and nodules must be considered. If the grain size is greater than approximately half the distance to the critical stress amplitude maximum at approximately the nodule radius, the stress amplitude to cross the second barrier can be less than the stress to cross the first barrier. Thus the strongest first barrier controls the fatigue limit. This is the case for a grain size of 25 μm (Figure 4). However, in a material with a smaller grain size, e.g. 10 μm , the stress amplitude necessary to cross the second furthest barrier at 20 μm is greater than the stress necessary to cross the first furthest barrier. This implies that

if the nodule radius is greater than approximately the grain size, the crack nuclei are not necessarily arrested at the first austenite grain boundary encountered. The length of arrested cracks can therefore be greater than the maximum austenite grain size. This is consistent with observations [Figure 1]. With decreasing grain size, there therefore is an increased likelihood that barriers encountered close to the critical stress amplitude maximum will arrest the crack nucleus. The effect of microstructure therefore becomes less significant as the grain size becomes small in comparison to the nodule radius. Similarly, the effect of microstructure diminishes for larger graphite nodules and the material behaves in a homogeneous manner.

The interactive effect between the austenite grain size and the nodule size on the fatigue limit was therefore predicted. The model assumes that if the distance to the maximum critical stress amplitude is greater than twice the grain size, the material is heterogeneous and fatigue limit is determined by the critical stress amplitude to overcome the microstructure barrier at the maximum distance of one grain from the nodule. For smaller grain size, the material is considered to be homogeneous and the maximum critical stress amplitude dictates the fatigue limit.

The results are shown in Figure 6, in comparison with test data [3] for an austempered ductile cast iron with an ausferrite grain size of approximately 25 μm . This data records the critical stress amplitude for failure, measured in rising load tension-tension fatigue tests performed in four-point bending at an R-ratio of 0.1. In each case, the size of the critical defects, which were graphite nodules or small shrinkage pores, was measured after failure.

The predicted fatigue limit is directly proportional to the assumed threshold value, ΔK_{th} . Good agreement was obtained for a grain size of 25 μm and a threshold value, ΔK_{th} , of 4.3 $\text{MPa}\sqrt{\text{m}}$. Agreement between the model and data could not be obtained for smaller or larger grain size using different thresholds. The model predicts that increasing grain size tends to decrease the fatigue limit, and the effect of grain size becomes negligible at larger nodule radius.

This proposed model for short crack nuclei in austempered ductile cast iron is consistent with literature observations of the fatigue behaviour of austempered ductile cast iron. Decreasing the size of the largest nucleating defect, for example by decreasing the graphite nodule size through increased nodule count [5-7], increasing graphite nodularity (i.e. reducing the maximum aspect ratio of the nodules) [8] or refining the austenite grain size through reduced austenitisation temperatures [9-13] all increase the fatigue limit. Increasing the volume fraction of retained and increased retained

austenite carbon content [9,11,7,14] are suggested to increase the intrinsic resistance to stage I crack growth, thus increasing the fatigue limit.

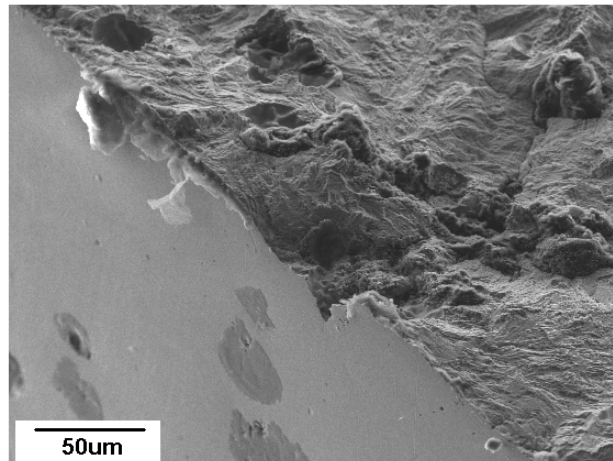


Figure 5: Fatigue failure nucleated at a graphite nodule [3]

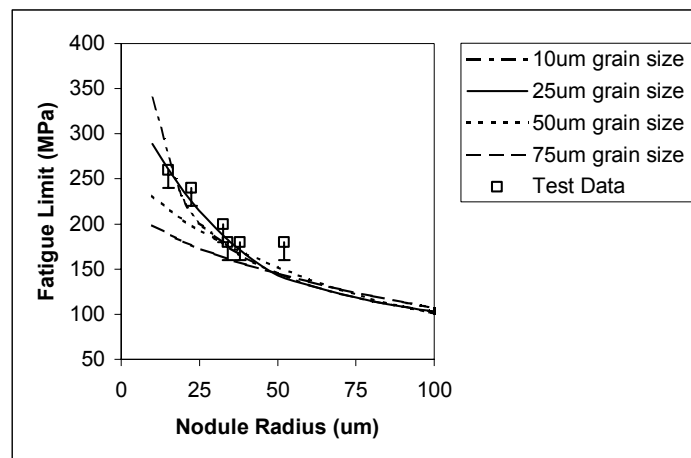


Figure 6: Effect of nodule radius and austenite grain size on the fatigue limit.

The proposed model predicts that the influence of the austenite grain size on the fatigue limit will diminish with increasing defect radius, as the grain size becomes small in comparison to the defect. However, the microstructure will also influence the fatigue endurance limit and fatigue life above the fatigue limit by crack retardation at barriers close to the defect, even if the initiating defect size is larger than the austenite grain size.

The model has been compared to test data from small specimens machined from castings. In all the specimens, failure nucleated at graphite nodules or similar sized shrinkage pores. Larger pores may occur in real castings, but their tip radii are similar to nodules, and of comparable size to the austenite grain size. Larger pores may also act as stress concentrators that act on adjacent nodules. Consequently, the fatigue behaviour of real components is also expected to be sensitive to graphite nodularity, nodule count and the matrix microstructure as predicted by the proposed model.

The range of defect sizes in a casting will control the statistical distribution of the fatigue limit or fatigue endurance limit. Increasing the specimen size will decrease the fatigue endurance limit by increasing the probability of occurrence of larger defects in the test population [15,16]. Work is now in progress to develop a microstructure fracture mechanics model for the relationship between the distribution of defect size and shape and the statistical distribution of the component fatigue limit in austempered ductile cast iron components. This will be tested against measurements of the fatigue limit, correlated with the initiating defect size and the microstructure.

CONCLUSIONS

- Stage I crystallographic microstructure short cracks, parallel to the austenite {111} slip planes, are nucleated at graphite nodules.
- The crack nuclei are retarded and arrested by microstructure barriers, such as ausferrite packet boundaries and prior austenite grain boundaries.
- The largest crack nucleus, which determines the fatigue limit or endurance limit, depends on the combination of largest defect and the prior austenite grain size.

ACKNOWLEDGEMENT

The authors would like to thank William Lee Foundry, Dronfield, for the supply of material and to acknowledge the financial support for study visits to the Manchester Materials Science Centre for HÇ from the British Council, TÜBİTAK (The Scientific and Technical Research Council of Turkey) and Dokuz Eylül University, Turkey and for MA-Z from the University of Aleppo, Syria.

REFERENCES

1. T.J. Marrow, H. Çetinel, C.S. Wang and H. Bayati (2000). *Heat Treat 2000*, 20th ASM Heat Treating Conference, St Louis, Missouri, USA. Vol 1, 528-534.
2. T.J. Marrow and H. Çetinel (2000). *Fatigue Fract. Engng Mater. Struct.* **23**, 425-434.
3. T.J. Marrow, H. Çetinel, M. Al-Zalmah, S. MacDonald, P.J. Withers and J. Walton (2002). *Fatigue Fract. Engng Mater. Struct.* **25**, in press.
4. B. Weiss, R. Stickler and A.F. Blom (1992). *Short Fatigue Cracks*, ESIS 13, pub. MEP, 423-430.
5. M. Sofue, S. Okada and T. Sasaki (1978). *AFS Transactions*, **86**, 173-183.
6. D. Venugopalan, K.L. Pilon and A. Alagarsamy (1980). *AFS Transactions*, **88**, 697-704.
7. J.F. Janowak, A. Alagarsamy and D. Venugopalan (1982). *AFS Transactions*, **90**, 511-518.
8. S.C. Lin, T.S. Lui and L.H. Chen (2000). *Metall. Mater. Trans. A* **31A**, 2193-2203.
9. P. Shanmugam, P. Prasad Rao, K. Rajendra Udupa and N. Venkataraman (1994). *J. Mater. Sci.* **29**, 4930-4940.
10. D. Krishnaraj, K.V. Rao and S. Seshan (1989). *AFS Trans.* **97**, 345-350.
11. M. Bahmani, R. Elliott and N. Varahram (1997). *J. Mater. Sci.*, **32**, 5383-5388.
12. C.K. Lin, P.K. Lai, T.S. Shih (1996). *Int. J. Fatigue*, **18**, 297-307.
13. L. Bartosiewicz, A.R. Krause, F.A. Alberts, I. Singh, S.K. Putatunda (1993). *Mater. Charac.* **30**, 221-234.
14. R.A. Harding (1986). *Metals and Materials*, **2**, 65-72.
15. S. Beretta and Y. Murakami (1998). *Fatigue Fract. Engng Mater. Struct.* **21**, 1049-1065.
16. C.K. Lin, W.J. Lee (1998). *Int. J. Fatigue*, **20**, 301-307.